WORKFLOW TO DESIGN AND DEPLOYMENT OF LOW-POWERED ELECTRIC VEHICLE

A SYNOPSIS

Submitted by

RAMACHANDRAN R
(Reg. No. 201711120)

in partial fulfillment for the award of the degree

of

DOCTOR OF PHILOSOPHY

DEPARTMENT OF INSTRUMENTATION AND CONTROL ENGINEERING
SCHOOL OF ELECTRONICS, ELECTRICAL AND BIO-MEDICAL TECHNOLOGY
KALASALINGAM ACADEMY OF RESEARCH AND EDUCATION

(DEEMED TO BE UNIVERSITY)

ANAND NAGAR, KRISHNANKOIL – 626 126

TAMIL NADU, INDIA

JUNE 2023

1. Introduction

The thesis will focus an optimization-driven approach to designing, validating, and deploying small electric vehicles (SEV). Downsizing electric vehicles could reduce cost, energy consumption, vehicle space and enhance mileage. However, designing SEV is a challenging problem due to its sensitivity to design choices from both performance and cost considerations. A design objective is to optimize both initial cost and increase mileage/charge by reducing dimensions, overcoming force-balance constraints, and selecting the right components. Optimizing the cost leads to the Multi-Objective-Mixed-Integer Nonlinear Programming (MO-MINLP) problem. Non-dominated sorting genetic algorithm 2 (NSGA 2) is used to solve this complex problem. The design outcomes are first verified through simulations on edge cases to avoid costly design modifications later during the SEV design cycle. The verification step involves testing vehicle performance on standard and user-defined drive cycles. Once the SEV passes the verification step, detailed vehicle design is performed wherein vehicle fabrication, electronic control unit, and controller tuning for the drive train is performed. This translates the vehicle design step to the final vehicle whose performance is validated through deployment.

Even though various approaches can be implemented in SEV design, an optimization-driven design approach that could reduce cost and improve range simultaneously is investigated in this study. In addition, a workflow that translates the design decisions to detailed design, avoiding costly iterations through suitable tool integration, is lacking in previous SEV design, This thesis addresses these gaps by:

(i) Constrained Multi-objective Optimization (C-MOP) method for optimizing capital cost and mileage of SEV for optimizing vehicle dimensions, perform component sizing and selection, and reduce effects of disturbances.

(ii) Propose a multi-disciplinary workflow to translate the design decisions to SEV that is verified for performance using simulation tools during design phase, perform detailed design.

(iii) A multi-objective ES-PID controller which maintains speed set-point and minimizes the torque ripples in the presence of load torque variations, yet is deployable on a low-cost hardware,

(iv) Stability and convergence analysis of the proposed controller, and

(v) Controller realization on a low-cost hardware and test results after deployment in EVs.

This requires a renewed look into the EV development whereby new types of vehicle design need to be introduced contrasting from existing ones such as traditional cars needs to be explored. In the Indian context, SEV occupying less space in roads and parking are very much desired. However, the current EVs being studied are designs that have been in vogue for a long-time. Moreover, such EV design should be complimented by electric drive train design that is cost effective and scalable to different applications (e.g., material handling in industries).

2. Literature Review

Optimization-driven approaches for EV design has received considerable attention recently in Grunditz et al. [1]. Available results can be broadly classified as: component-level design optimization discussed in Nemeth et al. [2], system level design presented by Du et al. [3] and sub-system level design explained in Ciceo et al. [4], and holistic designs are presented by Park and Park [5]. Component level designs focus on optimizing certain vehicle components such as motors that is discussed in Sun et al. [6]. In addition some studies focus on tuning vehicle performance parameters as mentioned in Hofman and Janssen [7]. Moreover, system or sub-system level design tries to optimize the holistic objectives. Vehicle optimization aims to find the best solution regarding single or multi-objectives. The most popular one is the energy consumption reported by Gao et al. [8]. In publications that deal with performance measures like speed and, acceleration or gradability are a common second objective. Further options are minimizing the features such as battery charge depletion is reported in Ahn et al. [9], active material cost is discussed in Fatemi et al. [10], aggregated weight, and also maximizing the features such as battery life and driving range. However, the aforementioned studies have their advantages and disadvantages. Arguably a vehicle designed for flat terrain may not be suited for high hill-climbing requirements. Nonetheless, they have not been applied to optimize the design and control of SEV, which have significantly different requirements.

Narrowing the scope towards previous research on the design of SEV, we identify the following contributions: Whilst simulation-based approaches reveal the capabilities of SEV, efforts have been made to optimize the design of the electric motor of SEV using finite-element modeling explained by Fatemi et al. [10] combined with gradient-

based is reviewed in Grunditz et al. [1]. A scaled-down electric vehicle was performed to verify the optimal input design method for fault identification in Park and Park [5]. However, these methods do not optimize the design and control of the full vehicle from a system-level perspective and deployment.

In the aspect of electrical design the control methods for BLDC motor, several control algorithms are proposed in the literature to control speed and minimize the load torque ripples. The fundamental approach is Pulse Width Modulation (PWM), wherein the ON/OFF time of the MOSFET switches are varied based on the error signal was explained by Zhou et al. [11]. However, it cannot handle load torque fluctuations. The Proportional Integral and Derivative (PID) controller, with its simple design, is a widely preferred choice for speed control. Further, these controllers can be deployed in low-cost control units. But they require proper tuning to handle the load disturbance. Fractional order PID controllers that retain the simple design of PID yet provide additional tuning parameters is proposed in Ganeshaperumal et al. [12]. However, it requires proper control parameter tuning for robust performance. Soft computing techniques such as fuzzy logic controllers discussed by Kahveci et al. [13], and artificial neural networks reported in Rubaai and Young [14] are investigated for speed control. Though these techniques provide human-like reasoning and can handle non-linear behaviors, they consume more memory.

To handle load torque fluctuations, adaptive control methods combining model-reference adaptive control and sliding mode approach was also proposed in Xia et al. [15], However, their implementation remains a challenge. Recently, optimization approaches have gained more significance in BLDC motor control due to their ability to provide performance and efficiency. Our objective is to combine the simplicity of PID with model-free optimization capability of extremum seeking control to provide a controller which is deployable on MCUs.

Summarizing, to the best of the authors' knowledge, there are no methodologies available to conduct such a holistic design, that the vehicle integration and deployment are considered in, systematic and computationally efficient manner, whilst accounting for their application-specific requirements.

3. Objectives

Our objective in the thesis are:

1. Constrained Multi-objective Optimization (C-MOP) method for optimizing capital cost and mileage of SEV for optimizing vehicle dimensions, perform component sizing and selection, and reduce effects of disturbances.
2. Propose a multi-disciplinary workflow to translate the design decisions to SEV that is verified for performance using simulation tools during design phase.
3. Performing detailed design including mechanical sub-system design and verfication.
4. Designing the Multi-Objective Extremum Seeking-Proportional Integral and Derivative (ES-PID) Controller for SEV.
5. Convergence and stability analysis for the ES-PID controller.
6. Realizing the control system with low-cost hardware for SEV.
7. Instrumentation sub-system design and verification.
8. Deploy the SEV and demonstrate its performance through test drives.

4. Research Problem

This section summarizes the workflow to design, verify and deploy of low-powered EV is shown in Figure 4.1. It has four phases: design, verification, detailed design and deployment. In the design phase, user requirements i.e., bounds on vehicle dimensions (e.g., maximum and minimum length) plus desired CAPEX and OPEX are the inputs that are fed through an JSON file. The user requirements entered through the JSON are given as inputs to the design tool whose objective is to minimize CAPEX and OPEX subject to force-balance constraints acting on the vehicle. As CAPEX is intrinsically linked to the components, their selection has also to be performed. To this extent, a component repository is created wherein the specifications in standard format are entered as JSON files. The design problem is also constrained by the force-balance equations of the vehicle that are nonlinear and non-convex. Therefore, the force-balance

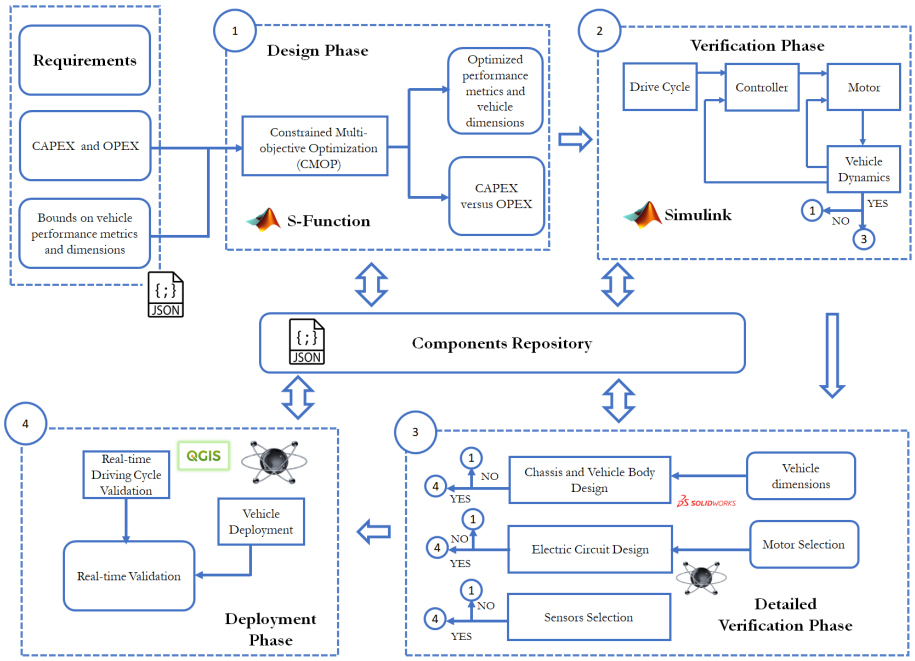

Figure 4.1: A detailed workflow for the small electric vehicle.

constraints alongside the component selection constraints makes the design problem a mixed integer nonlinear one. Besides, the CAPEX and OPEX are competing objectives, e.g., reducing initial battery cost means reducing EV range and vice-versa. As solving this constrained multi-objective nonlinear mixed integer optimization problem is overwhelming, meta-heuristic approach: the non-dominated sorting genetic algorithm II (NGSA II) is used within the design tool. The NSGA II is used mainly due to its ability to solve problems with integer constraints. In addition, sensitivity analysis is also performed wherein other design choices closer to the optimal solution are compared to understand the potential benefits. The design tool thus computes the optimal vehicle dimensions and selects the components that are the inputs to the verification phase.

In the verification phase, extensive simulations with vehicle dynamical equations is performed. Within the simulations standard drive cycles (e.g., FTP 75) are used as inputs to the vehicle dynamical equations and the vehicle performance is measured in terms of speed, battery SoC versus voltage, and vehicle acceleration are studied. Further, the vehicle performance over drive cycles reveal failure conditions such as vehicle not meeting specific speed or acceleration tracking. In worst case scenarios wherein the vehicle design fails the verification step, redesign is iterated again by modifying vehicle

dimensions bounds or constraints. Verified design and component selection is the input for the detailed design step phase.

In detailed design, different EV subsystems are designed. First, the mechanical system is designed by selecting suitable fabrication material and design improvisations to reduce force losses are introduced by using CAD models. Next, the electronic control unit (ECU) design problem is considered and it has two steps: hardware and software. The hardware design step consists of selecting suitable processor, power electronic components, signal processing units, sensor interfaces, and communication ports.

The hardware components and their signal outcomes are simulated in Proteus software to verify whether the hardware meets the design objectives. Similarly, software part of the ECU design addresses the control algorithm to maintain speed, interfacing sensors and other hardware, and driving the motor controller. In the ECU design, components are selected depending on the motor selection in the design phase and speed control algorithm is tuned to provide good tracking and regulatory performance. In our design, the proportional integral and derivative controller is selected due to its simplicity and performance. The controller tuning and implementation are also part of the detailed design phase. The third part of the detailed design is the selection and testing of sensors for noise, precision, and repeatability. The outcome of the detailed design phase are the mechanical fabrication design document and ECU design.

In the deployment phase, the mechanical design, ECU, and sensing systems are integrated within the EV and test rides are conducted. The studies are conducted to reveal valuable information on SoC, speed, acceleration, force losses, and performance metrics. In addition, the vehicle range, OPEX, and speed-control performance are also validated using trial runs. During trial runs Q-GIS is used for path-planning and integrated into the validation tests. Main advantage here is the verification being in-built during each phase to eliminate costly upgrades later on during the design cycle. In what follows, the different phases of the workflow are presented in greater detail.

4.1 Design Phase

Design is the first phase of the workflow wherein user requirements are the inputs in a JSON file. Bounds on vehicle dimensions and performance metrics (e.g., speed,

torque, etc.) are given as inputs in the form of JSON files. Similarly, the component repository as JSON files is the other input. The objective is to find the vehicle dimensions and components that optimize CAPEX and OPEX. The constraints are the vehicle dimensions, force-balance equations, performance limits, and component repository. The force-balance equations are nonlinear, and the component selection problem leads to integer decision variables. Moreover, as seen later, CAPEX and OPEX are competing objectives. This leads to a multi-objective mixed integer nonlinear programming (MO-MINLP) problem, which makes the design problem overwhelming. The next section gives the details of the MO-MINLP problem and constraints.

4.1.1 Cost based component sizing and control problem

The objective of the optimization problem is to minimize the vehicle CAPEX and OPEX defined as,

$$J_{tc} = C_{cap} + C_{op} \tag{1}$$

where C_{cap} is the CAPEX and C_{op} is OPEX, respectively. Suppose there are n different motors, battery chemistry, fabrication material available in the repository, the problem of selecting the components that meets the torque requirement along with wheel dimension is based on their CAPEX and modelled as:

$$\begin{aligned} C_{cap} = \;& C_m \cdot P_{m,max} + C_b \cdot E_{b,max} \\ & + C_f \cdot l_v \cdot b_v + C_w \cdot d_w \end{aligned} \tag{2}$$

where $P_{m,max}$ the maximum motor power output, $E_{b,max}$ denotes the maximum battery capacity, l_v and b_v are length and breadth of the vehicle, d_w the diameter of the wheel. Moreover, C_m and C_b, are the specific costs of motor and battery,respectively, and C_f and C_w are additional cost related to fabrication material and wheel of the vehicle. We define the OPEX as a function of battery according to

$$C_{op} = \Delta E_b \cdot C_{elec} \cdot \frac{R_{v,max}}{R_{v,cycle}} \tag{3}$$

where C_{elec} is the cost of electricity, $R_{v,max}$ is the distance that the vehicle can cover until the battery depth of discharge, $R_{v,cycle}$ is the distance covered in one driving cycle

and ΔEb is the difference in battery SoC defined as,

$$\Delta E_b = E_b(t_0) - E_b(t_{end}) \tag{4}$$

where t_0 and t_{end} denote the start and end times of the driving cycle, respectively.

4.1.2 Multi-objective Nonlinear Mixed Integer Programming

In this section, we present the optimization problem, summarizing the objective function and modeling constraints derived in the previous section. The problem of designing EV is a multi-objective optimization problem which is nonlinear and complex NP-hard problem. Therefore, solving this problem with mathematical programming techniques is a challenging task. We propose to use evolutionary-based computation techniques to optimize the design. The decision vector is,

$$X = [M_v, l_v, b_v, P_m, \omega_m, T_m, \eta_b, R_v, \sigma_1, \sigma_2]$$

should be computed by solving the following optimization model. To this extent, the optimization problem for the SEV is formulated as:

$$\begin{aligned}
\min_{X} \quad & J_{tc} \text{s.t. Equation } (1)-(4) \\
& M_{v,min} \leq M_v \leq M_{v,max} \\
& l_{v,min} \leq l_v \leq l_{v,max} \\
& b_{v,min} \leq b_v \leq b_{v,max} \\
& P_{m,min} \leq P_m \leq P_{m,max} \\
& \omega_{m,min} \leq \omega_m \leq \omega_{m,max} \\
& T_{m,min} \leq T_m \leq T_{m,max} \\
& \eta_{b,min} \leq \eta_b \leq \eta_{b,max} \\
& R_{v,min} \leq R_v \leq R_{v,max} \\
& \sigma_1 + \sigma_2 = 1
\end{aligned} \tag{5}$$

where σ_1 and σ_2 are weights associated with the objective functions.

The problem in (5) has multiple objectives and nonconvex constraints due to force balance equations, a computationally hard problem to solve. For this purpose, we now

present the detailed workflow for design, verification, and integration of SEV. The next section details about verification phase.

4.2 Verification Phase

Simulation models to verify vehicle performance are crucial for avoiding costly upgrades later down the design life-cycle. To this extent, the vehicle parameters and component selection are validated through simulation by modifying the Federal Test Procedure-75 (FTP-75) to match the maximum vehicle speed and repeating the cycle to study the energy consumption.

Simulations are performed by modeling the vehicle in MATLAB/Simulink, and the simulation procedure is automated by writing the MO-MINLP results into a text file that forms the input for the vehicle simulations. The motor parameters, battery, vehicle dimensions, and force calculations are fed to the Simulink using MATLAB. Design verification using simulations and FTP-75 drive cycles shows the vehicle's ability to track the reference speed. The simulation-driven verification helps validate design choices, studying vehicle range and battery performance for the design choice R_4. The detailed design is discussed in next section.

4.3 Detailed Design

Converting the computed optimal vehicle parameters to actual vehicle design requires detailed design. This involves designing the different subsystems: mechanical, electrical (motor controls), and instrumentation systems. The next step is choosing the appropriate ECU.

4.4 Electronic Control Unit Preliminaries

The in-wheel BLDC motors' armature has three winding a,b,c star connected which are excited by the inverter. Denoting current flowing through the windings as i_a,i_b,i_c, the equations describing BLDC motor phase voltage are (see, Sathyan et al. [16]):

$$V_j = R_j i_j(t) + L_j \frac{di_j(t)}{dt} + e_j(t), \forall j \in \{a,b,c\}, \forall t \in \mathbb{R}^+, \tag{6}$$

$$i_a(t) + i_b(t) + i_c(t) = 0, \qquad \forall t \in \mathbb{R}^+ \tag{7}$$

where V_j,R_j and L_j denote the j^{th} phase voltage, resistance and inductances, respectively. Similarly, e_j denotes the back-emf in our analysis. To simplify our model, we

assume: *(i)* resistances and inductance of the armature coil are identical, *(ii)* mutual inductance is negligible, and *(iii)* The applied voltage from the DC bus due to PWM is $\delta(t)V_{DC}/2$, where V_{DC} is the dc link voltage. These assumptions do not preclude adapting the results to more generic case. Equations governing back emf are:

$$\begin{aligned} e_a(t) &= K_b\ \omega_m(t)\ f(\theta_e), \\ e_b(t) &= K_b\ \omega_m(t)\ f(\theta_e - \frac{2\pi}{3}), \\ e_c(t) &= K_b\ \omega_m(t)\ f(\theta_e - \frac{4\pi}{3}), \forall t \in \mathbb{R}^+, \end{aligned} \tag{8}$$

where K_b and θ_e are the back emf constant in $\mathrm{V\,s\,rad^{-1}}$ and electrical displacement (rad), respectively. In addition, ω_m is the motor shaft angular velocity in $\mathrm{rad\,s^{-1}}$. The function $f(\theta_e)$ depends on the current rotor position and trapezoidal back emf waveform (see,Akin and Bhardwaj [17]). The total electromagnetic torque T_e is given by

$$T_e(t) = K_t \left[f(\theta_e) i_a(t) + f(\theta_e - \frac{2\pi}{3}) i_b(t) + f(\theta_e - \frac{4\pi}{3}) i_c(t) \right], \tag{9}$$

where K_t is the torque constant. One can observe that:

$$T_e(t) - T_l(t) = J\frac{d\omega_m(t)}{dt} + B\omega_m(t), \tag{10}$$

where $\omega_m = \frac{d\theta_m}{dt}$ and T_l denote the angular velocity in $\mathrm{rad\,s^{-1}}$ and load torque (N m), respectively. In addition, J and B denote the moment of inertia and damping coefficient. Equations (6)-(10) provide the detailed BLDC motor model. Suppose that commutation occurs between phase a and b, i.e., i_a has falling edge and i_b has raising edge, the slope, i.e., $-\frac{di_a(t)}{dt} = \frac{di_b(t)}{dt}$ and phase c is the non-commutating phase, thus for zero torque ripple, we have

$$\frac{di_c(t)}{dt} = \frac{di_a(t)}{dt} + \frac{di_b(t)}{dt} = 0 \tag{11}$$

Equation (11) gives the condition for zero torque ripple and equation (9) shows the effect of load-torque variations. **Our objective is to design a controller to track the speed set-point provided by the throttle with minimum torque ripple in the pres-**

ence of load-torque variations without incurring additional costs to existing PWM control technique. The objective to track reference speed is modelled as $O_1(t) = \|(\omega_m^{ref}(t) - \omega_m(t))\|_{\ell_2}$ and reducing torque ripple as $O_2(t) = \|\sum_{j\in n_c}(\frac{di_j(t)}{dt})\|_{\ell_0} \ \ \forall n_c \in \{a,b,c\}$, n_c is the index of commutating phases. In addition, ℓ_0 and ℓ_2 denote the 0-norm and 2-norm, respectively. The multi-objective ES-PID design problem aims to find the optimal $\delta(t) \ \ \forall t \in \mathbb{R}^+$ solving the following optimization problem:

$$\begin{aligned} &\min_{\delta(t)} \ [O_1(\delta(t)), O_2(\delta(t))] \\ &\text{s.t. Equations } (6)-(10), \\ &\delta^{min} \leq \delta(t) \leq \delta^{max}, \\ &\omega_m^{min} \leq \omega_m(t) \leq \omega_m^{max}, \end{aligned} \tag{12}$$

In addition, $\delta^{min}, \delta^{max}, \omega_m^{min}$ and ω_m^{max} denote the bounds on the duty cycle and motor speed, respectively. Clearly, (12) is a multi-objective, nonlinear, non-convex and continuous time optimization problem. The multiple objectives are: track reference speed and reduce the torque ripple by proper choice of the duty-cycle. The nonlinearities and nonconvex constraints are due to BLDC model equations and the ℓ_0 constraint. While solving the problem is challenging, the need to deploy in simple hardware adds another complex dimension as solving such optimization requires specialised hardware for controller realisation. On the other hand, using BLDC motor has significant torque ripple due to trapezoidal commutation and tracking with load torque fluctuations is also difficult. Consequently, deploying controller will necessitate specialized hardware to solve the complex optimization model.In what follows we describe an approach to design a controller overcoming the challenges.

4.4.1 Multi-Objective ES-PID Controller for SEV

This section presents a Multi-objective ES-PID controller for EV. To tune the parameters we use the ES-algorithm, a model-free optimization approach which computes the gradient without using functional differentiation. The ESCs' model-free approach is also important considering the fact that load torque variations in EVs are quite frequent and traditional approach is to use models or estimators. Using such techniques for low-power electric vehicles is infeasible due to hardware costs. Therefore, a model-free

approach will alleviate the need for modelling or estimation on load torque, yet provide desirable performance. More details about ES-algorithm can be found in Ariyur and Krstic [18]. Since the measurements are used in the computations, the ES-algorithm handles the nonlinear constraints imposed by the dynamical equations (6)–(10) inherently. To handle the limits on the control signal and speed computation, we use a projection operator given by

$$Proj(\omega_m, \omega_m^{min}, \omega_m^{max}) = \begin{cases} \omega_m^{max}, & \text{if } \omega_m > \omega_m^{max} \\ \omega_m, & \text{if } \omega_m^{min} \leq \omega_m \leq \omega^{max} \\ \omega_m^{min}, & \text{if } \omega_m < \omega_m^{min} \end{cases}$$

The ES-algorithm has two shortcomings, they are: *(i)* slow convergence and *(ii)* frequent retuning. To overcome these shortcomings, we make two modifications: *(i)* hot-starting and *(ii)* event-based triggers for retuning. By hot-starting, we mean initializing the PID parameters using optimal PID parameters computed from PID tune tool from MATLAB/Simulink which helps to achieve faster convergence.

Moreover, restricting the search space within feasible values could help improve the convergence. To this extent, hardware in the loop (HIL) simulations with BLDC motor model to compute the controller parameters is performed and the limits on the controller gains are computed using simulations. This provides nominal parameters and search space as well which could be computed online based on load-torque variations. The nominal PID parameters are computed using the ES-PID with optimal PID controller parameters as the starting point. Similarly, the bounds on the PID parameters are computed using HIL simulations which is illustrated later in this section. This aspect of the HIL based hot-starting is illustrated in Figure 4.2.

Second, to avoid frequent retuning, we propose two switches. The first switch is based on the average time over error threshold (τ_{av}) in a given interval and is given by $\tau_{av} = \frac{t_i}{T_r},\ t_i \in \{1,2,\ldots,T_r\}$ where T_r is the time-period over which the threshold deviations are computed and it usually varies between 4-5 sampling intervals. This switch computes the average speed variations within a given time to trigger ESC. Second switch models the torque-ripple over the time-period T_r (second term in (14)), and is computed as $\sigma_n = \frac{\|(\Delta i_j(k)\|_{\ell_0}}{T_r},\ \forall k \in \{1,2,\ldots,T_r\}, \forall j \in n_c$. Still the objective function

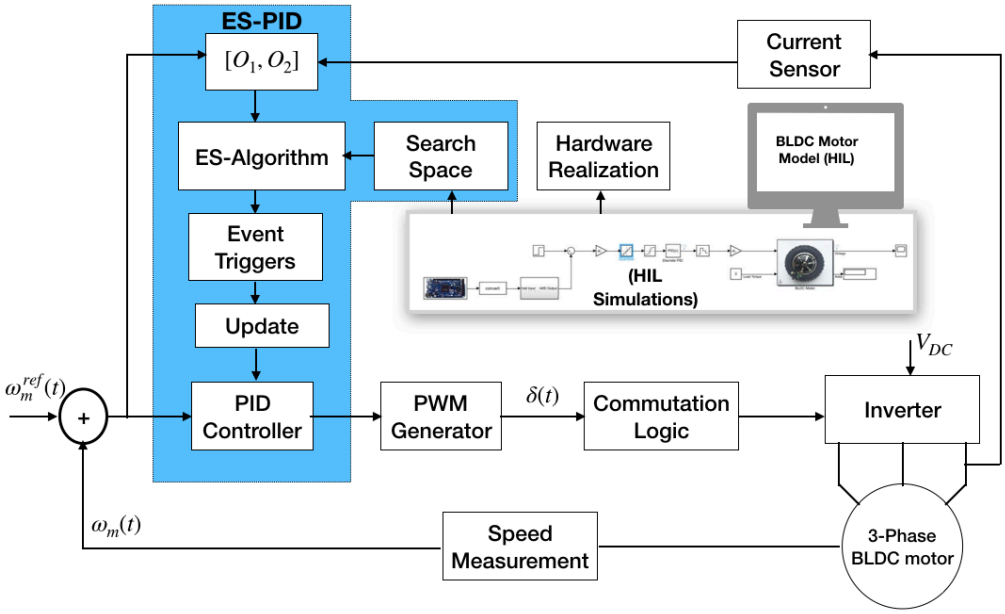

Figure 4.2: Block diagram of ESC

is non-convex due to the ℓ_0 term which needs to be relaxed. In what follows, we present a convex relaxation which will provide an easy way to design the ES-PID controller and the design equations are also presented.

4.4.2 ES-PID Controller

Let $\boldsymbol{\Phi} = [\phi_1, \phi_2, \phi_3] = [k_p, k_i, k_d]^T$ be the decision variables of the optimization problem in (12). To remove the ℓ_0 part of the objective function, we employ the relaxation in (13).

$$O(\boldsymbol{\Phi}) = \left(\liminf_{t\to\infty} \frac{1}{T} \kappa_1 \int_t^{t+T} \varepsilon^2(\tau) d\tau \right) + \kappa_2 \int_t^{t+T} i_j(\tau) d\tau, \quad \forall j \in n_c \tag{13}$$

where κ_1 and κ_2 are the weighting factors and T is the sampling period. In addition, ε models the error between the speed set-point and actual-speed of the BLDC motor. The relaxation is obtained by observing that $\int_a^b f(x)dx = f(b) - f(a)$ and $\frac{di_j}{dt} = \frac{i_j(k) - i_j(k-1)}{T}$.

Remark 1. *Minimizing the integral of the second term in the equation* (13) *is approximately reducing the* ℓ_0 *terms of the current variations as the sum of the currents at any given time is equal to zero from* (7).

Remark 2. *The first term in $J(\boldsymbol{\Phi})$ tries to reduce the error between set and actual speed, whereas the second term tries to minimize the torque ripple. Weighing parameters κ_1 and κ_2 can be used to normalize the objective and their choices may modify the system performance.*

Remark 3. *The objective function in* (13) *cannot be measured online. To overcome this, we introduce the following cost:*

$$O_k(\boldsymbol{\Phi}) = \kappa_1 \frac{1}{T} \sum_{k=T}^{(k+1)T} \varepsilon^2(k) + \kappa_2 \mid \sum_{j \in n_c} \sum_{k=T}^{(k+1)T} \Delta i_j(k) \mid, \tag{14}$$

where $\Delta i_j = \frac{i_j(k) - i_j(k-1)}{T}, \ \ \forall j \in n_c$.

Remark 4. *Still the optimization objective in* (14) *is non-convex due to the second term. To relax it as a convex constraint, we introduce the following relaxation:*

$$\begin{aligned} O_k(\boldsymbol{\Phi}) &= \kappa_1 \frac{1}{T} \sum_{k=T}^{(k+1)T} \varepsilon^2(k) + \kappa_2 \Psi \\ s.t. \sum_{j \in n_c} \sum_{k=T}^{(k+1)T} \Delta i_j(k) &\leq \Psi, \\ \sum_{j \in n_c} \sum_{k=T}^{(k+1)T} \Delta i_j(k) &\geq \Psi, \end{aligned} \tag{15}$$

where Ψ *is a scalar which is an epigraph for* $\sum_{j \in n_c} \sum_{k=T}^{(k+1)T}$ $\Delta i_j(k)$. *In addition* κ_1 *and* κ_2 *are scalars which are selected depending the maximum speed of the BLDC motor. For low speed-BLDC motors, the torque ripple is high and therefore,* $\kappa_2 \geq \kappa_1$ *and for high-speed motors desiring tracking performance* $\kappa_1 \geq \kappa_2$. *In general, by selecting* $\kappa_1 = \kappa_2$, *nominal performance could be achieved.*

Remark 5. *The cost function in* (13) *provides a mapping between tuning parameter* $\boldsymbol{\Phi}$. *To reduce the search space we introduce the set:* $\mathscr{T} :=$

$\left\{(k_p, k_i, k_d) :\mid \left[k_p^{min} k_p^{max}\right], \left[k_i^{min} k_i^{max}\right], \left[k_d^{min} k_d^{max}\right]\right\}$.

Clearly, the objective function in (13) *should be bounded for any value within the set* $\mathscr{T}$ *to avoid unstable performance.*

Then the PID parameters ϕ are adjusted based by computing the gradient using the following equations Killingsworth and Krstic [19]:

$$\zeta_i(j) = -h\zeta_i(j-1) + O(\phi_i(j-1)) \tag{16}$$
$$\hat{\phi}_i(j+1) = \hat{\phi}_i(j) - \gamma_i\ \alpha_i cos(\mu_i k)[O(\phi_i(j)) - (1+h)\zeta_i(j)]$$
$$\phi_i(j+1) = \hat{\phi}_i(j+1) + \alpha_i cos(\mu_i(j+1)) \quad \forall i \in \{k_p, k_i, k_d\}$$

where $j \in \{1,2,\ldots,n_i\}, n_i, \zeta_i, \alpha_i, \gamma_i$ and μ_i are the iteration count, maximum iterations and positive scalars which are selected as in Killingsworth and Krstic [19]. Here $\gamma_i < 1$ is the adaptation gain, μ_i modulation frequency which is selected such that $\mu_i = a^i\pi, 0 < a < 1$, α_i is the perturbation amplitude, and h is the high-pass filter parameter with $0 < h < 1$. Readers are referred to Killingsworth and Krstic [19] and references for more details on ES-PID controller. The ES-PID controller is a model free optimization approach which is suitable for our application. However, the optimization is very slow and real-time adaptation is quite difficult. Furthermore, realization aspects of ES-PID controller on low-cost embedded platform for EV applications has not been fully explored to our best knowledge. So the next step is to study implementation aspects of ES-PID.

4.5 Integration and Deployment

The final step is the optimal vehicle design computed by solving the CMOP problem in (5) should be converted into an actual design. Vehicle weight should be minimized in this sense, so various alternatives such as aluminum, carbon steel, steel, and iron were taken into account. Aspects such as weight, machinability, welding capability, protection, and re-usability were taken into account. Carbon steel is chosen because of its low weight, readability with these choices and cost as a criterion. A back-driven configuration with two rear wheel motors is chosen. The next move is to fix the front differential drive and a customized design is chosen as the cost of off-the-shelf ones was high.

5. Organization of Thesis

The outline of thesis is as follows:

1. Chapter 1: Introduction
   - Overview
   - Motivation
   - Research Scope

- Summary of the Thesis
- Major Contributions

2. Chapter 2: Literature Survey
   - Optimization Algorithm
   - Control Methods

3. Chapter 3: Design Phase
   - Chapter Overview
   - Component Selection
   - Overview of NSGA II
   - Optimal Vehicle Design Parameters
   - Sensitivity Analysis

4. Chapter 4: Verification Phase
   - Chapter Overview
   - Vehicle Simulation
   - Verification

5. Chapter 5: Detailed Design
   - Chapter Overview
   - Mechanical System Design
   - Electronic Control Unit Design
   - Multi-Objective ES-PID Controller for SEV
   - Hardware-in-the-Loop for Designing ES-PID
   - Convergence and stability
   - Comparison of speed tracking performance
   - Comparison of torque variations
   - Instrumentation System Design

6. Chapter 6: Integration and Deployment
   - Chapter Overview
   - Fabrication of low-powered EV
   - Deployment Results and Discussion
   - Conclusion

7. Chapter 7: Conclusion and Future Directions
   - Conclusion
   - Future Directions

6. References

1. E. A. Grunditz, T. Thiringer, N. Saadat, Acceleration, drive cycle efficiency, and cost tradeoffs for scaled electric vehicle drive system, *IEEE Transactions on Industry Applications,* **56** (2020), 3020–3033.

2. T. Nemeth, A. Bubert, J. N. Becker, R. W. De Doncker, D. U. Sauer, A simulation platform for optimization of electric vehicles with modular drivetrain topologies, *IEEE Transactions on Transportation Electrification,* **4** (2018), 888–900.

3. W. Du, S. Zhao, L. Jin, J. Gao, Z. Zheng, Optimization design and performance comparison of different powertrains of electric vehicles, *Mechanism and Machine Theory*, **156** (2021), 104**–**143.

4. S. Ciceo, C. T. Faria, J. Gyselinck, C. Martis, Multi-attribute, system-level design process for automotive powertrain electric drives: An integrated approach, *SAE International Journal of Alternative Powertrains,* **7** (2018), 117–128.

5. J. Park, Y. Park, Experimental verification of fault identification for over actuated system with a scaled-down electric vehicle, *International Journal of Automotive Technology*, **21** (2020), 1037–1045.

6. X. Sun, Z. Shi, Y. Cai, G. Lei, Y. Guo, J. Zhu, Driving-cycle-oriented design optimization of a permanent magnet hub motor drive system for a four-wheel-drive electric vehicle, *IEEE Transactions on Transportation Electrification,* **6** (2020), 1115–1125.

7. T. Hofman, N. Janssen, Integrated design optimization of the transmission system and vehicle control for electric vehicles, *IFAC-Papers On Line*, **50** (2017), 10072–10077.

8. Z. Gao, T. LaClair, S. Ou, S. Huff, G. Wu, P. Hao, K. Boriboonsomsin, M. Barth, Evaluation of electric vehicle component performance over eco-driving cycles, *Energy,* **172** (2019), 823–839.

9. K. Ahn, A. E. Bayrak, P. Y. Papalambros, Electric vehicle design optimization: Integration of a high-fidelity interior-permanent-magnet motor model, *IEEE Trans- actions on Vehicular Technology*, **64** (2014), 3870–3877.

10. A. Fatemi, N. A. Demerdash, T. W. Nehl, D. M. Ionel, Large-scale design optimization of pm machines over a target operating cycle, *IEEE Transactions on Industry Applications,* **52** (2016), 3772–3782.

11. X. Zhou, Y. Zhou, C. Peng, F. Zeng, X. Song, Sensorless BLDC motor commutation point detection and phase deviation correction method, *IEEE Transactions on Power Electronics*, **34** (2018), 5880–5892.

12. D. Ganeshaperumal, N. Muthukumar, K. Ramkumar, S. Srinivasan, B. Subathra, Optimal fractional controller design methodology for electric drive train, *International Journal of Electric and Hybrid Vehicles*, **8** (2016), 335–350.

13. H. Kahveci, H. Okumus, M. Ekici, Improved brushless DC motor speed controller with digital signal processor, *Electronics letters*, **50** (2014), 864–866.

14. A. Rubaai, P. Young, Hardware/software implementation of fuzzy-neural-network self-learning control methods for brushless DC motor drives, *IEEE Transactions on Industry Applications*, **52** (2015), 414–424.

15. C. Xia, G. Jiang, W. Chen, T. Shi, Switching-gain adaptation current control for brushless DC motors, *IEEE Transactions on Industrial Electronics*, **63** (2015), 2044–2052.

16. A. Sathyan, N. Milivojevic, Y.-J. Lee, M. Krishnamurthy, A. Emadi, An FPGA-based novel digital PWM control scheme for BLDC motor drives, *IEEE Transactions on Industrial Electronics*, **56** (2009), 3040–3049.

17. B. Akin, M. Bhardwaj, Trapezoidal control of BLDC motors using hall effect sensors, *Texas instruments* (2010).

18. K. B. Ariyur, M. Krstic, Real-time optimization by extremum-seeking control, *John Wiley & Sons*, (2003).

19. N. J. Killingsworth, M. Krstic, PID tuning using extremum seeking: online, model-free performance optimization, *IEEE Control Systems Magazine*, **26** (2006), 70–79.

7. List of Publications

1. **R. Ramachandran**, D. Ganeshaperumal, B. Subathra, Design Optimisation and experimental verification of small electric vehicles, *Journal of Environmental Protection and Ecology*, **24** (2023), 126-135.
2. **R. Ramachandran**, D. Ganeshaperumal, S. Seshadhri, B. Subathra, P. Muthuvel, B. Korkut, Real-time extremum seeking controller for brushless DC hub motors in electric vehicles, *IET Electric Power Applications*, **14** (2020), 2438-2449.
3. **R. Ramaraj**, D. Ganeshaperumal, B. Subathra, K. Renu, Model-Based Hardware-in-the-Loop Closed- Loop Control of Brushless Direct Current Motor in Electric Vehicle Applications, *Flexible Electronics for Electric Vehicles: Select Proceedings of FlexEV—2021*, *Springer Nature Singapore*, **863** (2022), 59-72.